Development of Subsonic Single Aft Engine (SUSAN) Attritable Research Vehicle (SARV) Wing Structure

Lilia R. Miller[1]

NASA Glenn Research Center, Brook Park, Ohio 44135

This paper introduces a high-level overview of the design and development of the SUbsonic Single Aft eNgine (SUSAN) Attritable Research Vehicle (SARV) wing structure. Unique design considerations were made for the structural layout of the wing to include storage for batteries, distributed electric engines, and the requirement for the wing to be shippable in a cargo box. The wing structure development process will be discussed including the wing internal structure design evolution, the fabrication of the manufacturing demonstration vehicle, wing outer mold line design, integration of wing internal structure and wing skins, and finally integration of the wing with the fuselage structure. Additionally, the development of the wing skin design will be discussed while highlighting the wing skin manufacturing demonstration panels as well as composite testing for material characterization purposes.

I. Nomenclature

FoS	= factor of safety
MoS	= margin of safety
SUSAN	= Subsonic Single Aft Engine
SARV	= SUSAN Attritable Research Vehicle
SL	= sea level
S_{ref}	= reference surface area
W	= maximum takeoff weight
ρ_{ref}	= reference air density
V_{ref}	= reference speed

II. Introduction

The SUbsonic Single Aft eNgine (SUSAN) Attritable Research Vehicle (SARV) is a 25% direct scale down of the SUSAN full-scale 180-passenger vehicle outer mold line (OML). It supports the full-scale SUSAN vehicle through serving as a remotely piloted flying research testbed for the integrated flight, propulsion, and controls architecture of the SUSAN aircraft. This allows the project to incrementally validate novel design concepts and reduce technical risk. This paper will focus on the design and development of the flight wing structure for the SUSAN SARV. This will include the wing substructure as well as composite skins. Focus will be given to key takeaways from the development process and how each step feeds into validating the structure.

III. Wing Development Process

This section outlines the processes and activities performed and the development of the SARV wing structure. Many design iterations were performed to take into consideration unique design aspects, packaging, and structural integration. In addition to these design and analysis progressions, further activities included development of the composite wing skin design. In support of this effort, testing was carried out to characterize wing skin properties to feed into analytical models.

Part of the wing development process included manufacturability considerations. To help understand what aspects of the wing design carried manufacturing limitations, the design was updated for buildability and

[1] AST, Structural Mechanics, Structural Mechanics Branch, AIAA Member

constructed in house at NASA Glenn Research Center. In completing this manufacturing demonstration vehicle, the team compiled lessons learned to feed into the next wing design iteration.

IV. Unique Design Considerations

The SUSAN SARV structure is constrained by a few unique design considerations in addition to the requirement that the vehicle must be low cost and quick to manufacture. The first of these constraints includes the battery packaging in the wing. This can impact the typical spar/rib layout of the wing as more space is needed for both storage of the batteries as well as considerations for thermal management systems. Additionally, this will impact the typical wing loads an aircraft will see as having both fuel and electric packs in the wings will create a landing weight that is closer to the takeoff weight. Further unique considerations include integrating the distributed propulsion onto the wing structure. It is expected that the wing mounted electric engines will not only impact the control surfaces and the loads they see but also create more distributed loads across the wings as opposed to single nacelles of typical aircraft. Lastly, there is a requirement that the SARV structure must be transportable. Wings, fuselage, and tail section will be assembled on site after arriving in a common shipping container. Part of this requirement includes wings which can be removed and reattached easily, while being able to carry the aerodynamic loads seen in flight across a separable joint.

V. Wing Internal Structure Design Iteration

The SARV wing internal structure went through many design evolutions. Much of the design evolutions centered around the battery packaging in the wing and included utilizing the forward spar as a structural battery box member, having nonstructural battery boxes as storage in the wing, and having rib – like battery boxes adding additional stiffness in the wing shown in Figure 1 below.

Analysis was iteratively performed to narrow down design details for the ribs, spars, and battery boxes. For the purposes of this paper, this section will focus on iterations performed for the latest spar and rib layout. Finite element analysis was performed to check the internal structure margins of safety under flight loading environments and determine weight savings opportunities.

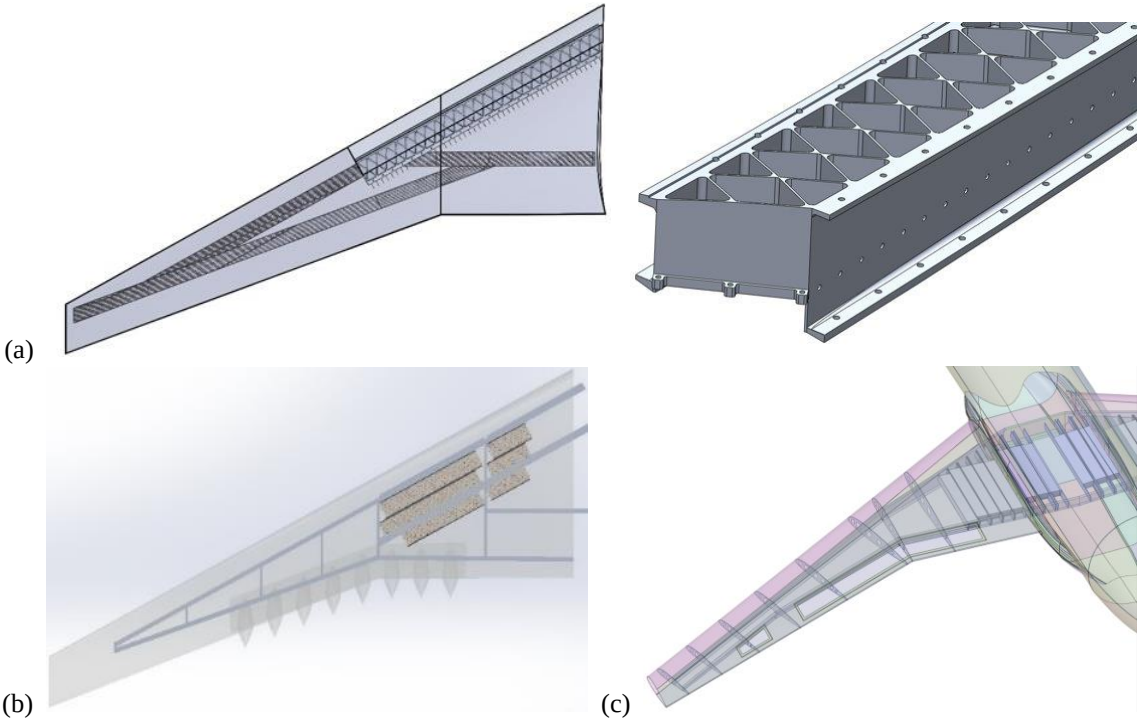

Fig. 1. Example design evolution of battery packaging in the wing. (a) Battery box wing spar layout and closeup view of battery box spar. (b) Non-structural battery box storage. (c) Structural rib-like battery boxes.

A. Wing Structure Design

The design of the wing structure utilizes tapered c- channels at both the forward and aft spar locations, with the forward spar located at the quarter cord location. Part of the design effort is to develop the wing torque box to manage wing flutter. The torque box is the region between the spars bounded by the upper and lower skins and stabilized by the ribs. The channels of both these wings meet in the center of the aircraft and form the wing box. The ribs are designed such that they provide support for both the leading and trailing edge of the wing. The ribs also include cutouts for the forward and aft spars to nest within. Considerations are made for battery storage within the wing, and battery boxes that serve as structural members are attached between the forward and aft spar of the wing box as well as the first compartment location of the wing. Additionally, composite wing skin geometry is included here with the intention of attaching the wing skin to the ribs. The layout of this design can be referenced below in Figure 2. This current design does not yet include geometric considerations for landing gear, wing mounted motors, or control surfaces.

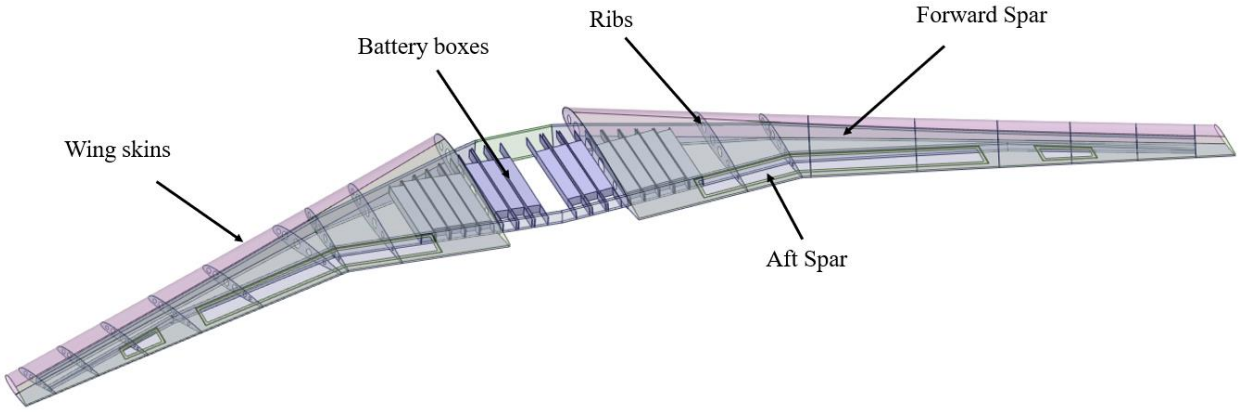

Fig. 2. Diagram of SARV wing structure design.

B. Wing Structure Finite Element Analysis

Load cases for the wing structure were taken from Table 1 [1]. Each load case was looked at to determine the controlling worst case loads on the wing. Landing loads were not considered in this analysis as landing gear geometry is not yet included. Preliminary analysis showed symmetric pull up as the controlling case for the wing breakout model.

Table 1. Flight Maneuvers that Produce Significant Flight Loads [1]

Aircraft Component	Maneuvers that normally produce high external loads
Wing	Symmetric pull-up
	G loaded rolling conditions
	Landing
	Symmetric vertical gust
	Head on Gust

This load case includes 3.75g load factor with the wings set at an 11.054 deg angle of attack (AoA) as well as aerodynamic loads on the wing. Computational fluid dynamics (CFD) simulations were used to determine the approximation of aerodynamic loads on the outer mold line (OML) of the wing. The wing case was run through steady Reynolds-averaged Navier–Stokes (RANS) calculations using Launch Ascent and Vehicle Aerodynamics (LAVA) curvilinear solver [2]. Flight conditions used in the computation of aerodynamic loads are summarized in Table 2.

Table 2. Flight Conditions

Condition	Value
SL	0 ft
H_C	10,000 ft
V_C	130 kt (150 mph)
W	1,500 lb.
S_{ref}	81.125 ft^2
V_{ref}	225.61 ft/s
ρ_{ref}	0.001755 $slugs/ft^3$

The breakout model of the wing was constructed in FEMAP 2022.2. Shell elements were used to quickly iterate section thicknesses of the design. Figure 3 shows the coincident mesh connection of wing members as detailed connections are not yet included in the geometry.

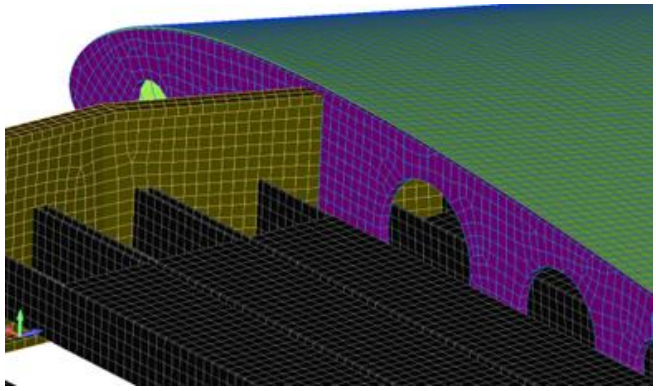

Fig. 3. Coincident mesh connections in FEMAP wing model.

The first iteration of the analysis utilized aluminum 6061 material for both these spars and ribs with a section thickness of 0.375 inches. This resulted in a fairly heavy wing with high margins of safety, and plenty of room to optimize the structure and cut weight. Analysis iterations followed this and looked at both cutting the section thickness of the spars and ribs as well as utilizing aluminum 7075 material. Examples of the Von-Mises stress results on the ribs and spars of design iteration 4 is shown in Figure 4 below. The analysis iterations are summarized in Table 3 below and ultimately cut the weight per wing by 64 pounds while maintaining positive margins of safety.

Table 3. Summary of Wing Design & Analysis Iterations

Design Iteration	Component Location	Material	Section Thickness	Weight Per Wing*	Yield MoS	Ultimate MoS
1	Spars	AL 6061	0.375 in.	97 lb.	3.67	1.61
	Ribs	AL 6061	0.375 in.		2.68	1.15
2	Spars	AL 6061	0.25 in.	65 lb.	1.40	0.41
	Ribs	AL 6061	0.25 in.		1.76	0.51
3	Spars	AL 6061	0.19 in.	49.6 lb.	0.63	0.04
	Ribs	AL 6061	0.19 in.		1.38	0.24
4	Spars	AL 7075	0.125 in.	33.3 lb.	0.77	0.07
	Ribs	AL 7075	0.125 in.		1.86	0.59

* Weight per wing inclusive of spars and ribs only

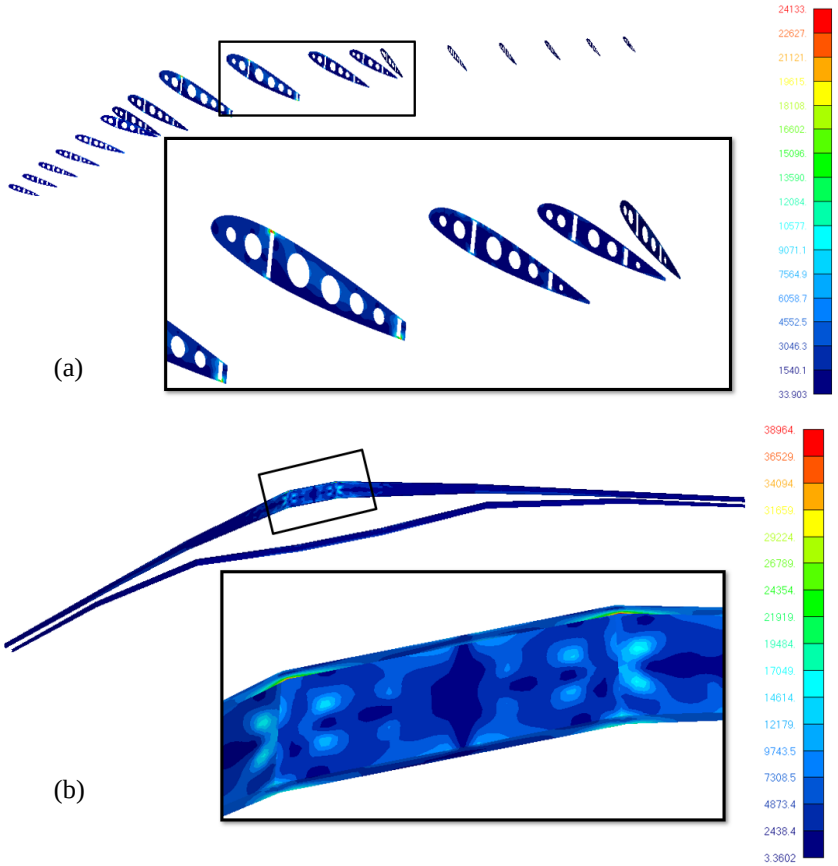

Fig. 4. Von-Mises stress results on the (a) ribs and (b) spars of design iteration 4.

Calculated *MoS* follow NASA standards as detailed in NASA-STD-5001b **Error! Reference source not found.**:

$$MoS = \frac{Allowable\ load\ (\text{yield or ultimate})}{Limit\ load * FoS\ (\text{yield or ultimate})} - 1 \quad (1)$$

Following this equation, positive margins of safety must be met on all components in both yield and ultimate load conditions. Additionally, following standards and requirements for the 25%-scale SUSAN flight research vehicle as outlined by Miller et al., *MoS* computations adhere to the *FoS* requirements summarized in Table 4 below. Structural components will be verified by proof tests up to 120% design limit load, and therefore, analysis utilizes a *FoS* of 1.0 in yield, and 1.8 in ultimate.

Table 4 NASA Armstrong Factors of Safety (Error! Reference source not found. **Revision A)**

Factor of Safety	Material	Condition
2.25 ~ 3.00	Composite	Structure verified by analysis along with building-block approach* (2.25 with well-established building block approach, higher *FoS* for limited building-block approach employed).
2.25	Metal	Structures verified by analysis only
1.80	Metal or composite	Structure verified by proof tests up to 120% design limit load
1.50	Metal or composite	Structural proof test plus full flight instrumentation
Additional 1.15	Joints and fittings	Where failure of one fastener, pin, or lug could result in loss of a component

*Building-block approach employs testing of certain design features at each of the complexity levels (starting with coupons, elements to design, detailed design locations, subcomponents, and components), which is then used to validate the design.

C. Manufacturing Demonstration Structure

Following the flight wing analysis iterations, a manufacturing demonstration vehicle was considered. The purpose of this demonstration structure was to take the simplified flight wing design and incorporate manufacturing considerations to come up with a wing design that could be build in-house at NASA Glenn Research Center. In addition to focusing on the wing, this demonstration vehicle also featured the fully built fuselage design, T-tail, engine mount, and static landing gear, all of which can be seen in Figures 5 and 6.

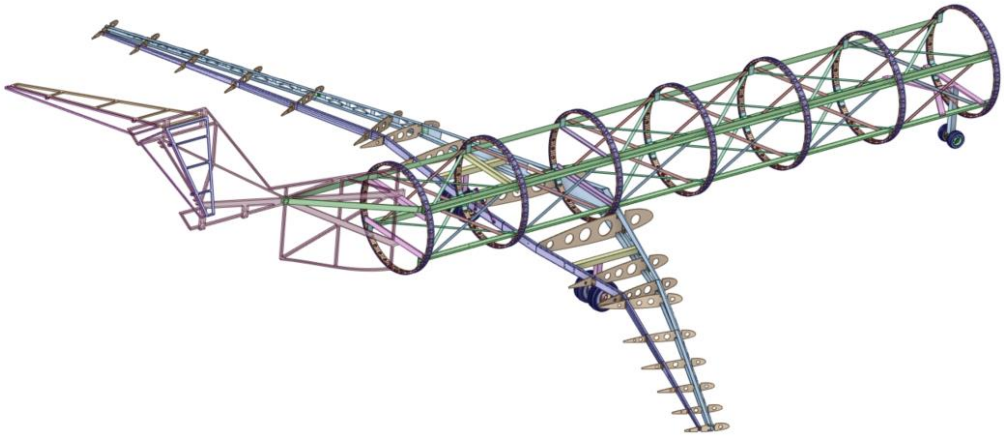

Fig. 5. Geometry of 25% manufacturing demonstration vehicle.

Fig. 6. Completed fabrication of 25% manufacturing demonstration vehicle.

In the initial simplified wing design, the spars fed through slotted holes in the ribs. Manufacturing of the spars utilized bending aluminum sheet metal in order to create the c-channels. With large bend radii of the spars, the ribs were no longer large enough to feed the spars through and a redesign of the ribs was completed to resolve the manufacturing limitations. Ribs were split into three pieces to represent the leading edge, trailing edge, and forward spar to aft spar connection in the middle as shown in Figure 7 below.

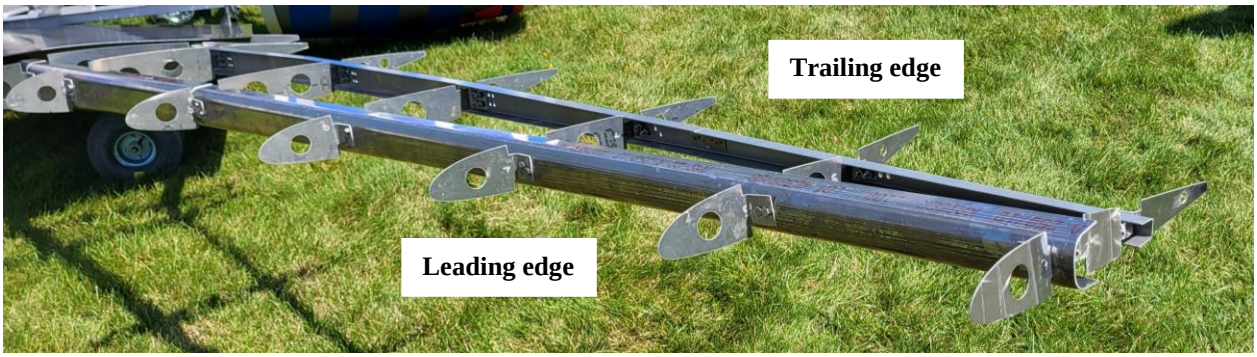

Fig 7. Close up of rib design for manufacturing demonstration vehicle.

Many lessons learned were taken away from this build including:

- Tooling limitations
- Bend radius limitations of different materials
- Cracking prone from certain bend radii
- Stiffness issues with built wing – not stiff enough
- Detachable wing not as quick to disassemble from fuselage as design intention

VI. Wing Outer Mold Line Design Evolution

The outer mold line (OML) is a 25% scale down from the full-scale SUSAN vehicle OML. This section will cover the wing skin design evolution. Manufacturing demonstration panels as well as wing skin design will be introduced. This section will also discuss the composite testing for material characterization.

A. Wing Skin Design

The SUSAN SARV wing skin design consists of a mix of two material systems and foam core used in the composite configuration:

- Fibreglast 2363 – Plain weave carbon fiber (0.005” thick)
- Fibreglast 530 – Plain weave carbon fiber (0.009” thick)
- Rohacell IG31 Foam (0.125” thick)

Figure 8 below highlights the wing skin cross sectional view where the main acreage region of the panel consists of a foam core center with 2 plies on either side. 16-ply build-up regions serve as hard points on the sides of the panel where the composite skin will fasten to the ribs of the wing structure.

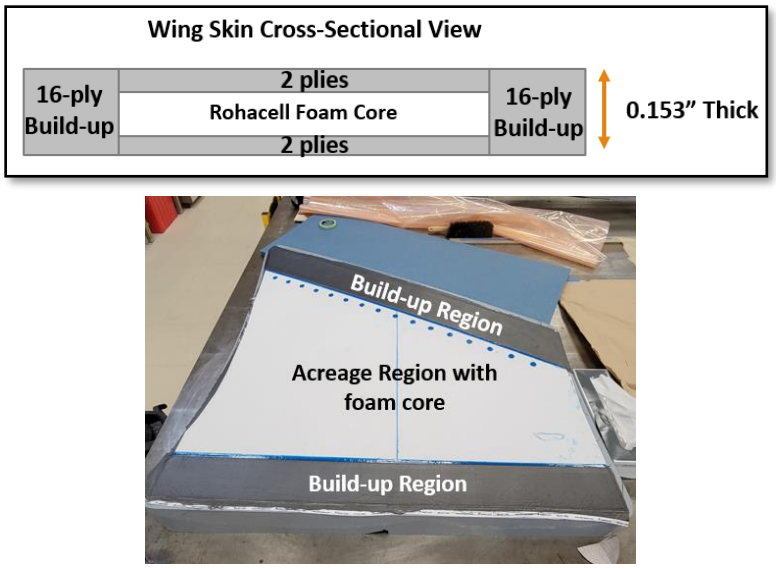

Fig. 8. Wing skin cross sectional and internal view of build.

B. Composite Testing

Quarter-scaled composite wing skin panels, shown below in Figure 9 were designed and built to demonstrate the manufacturing process. With no SUSAN wing skin specific test data to back up the predicted structural performance, the laminate level structural performance is not well known. To develop the analytical capability to predict structural behavior including stress, deformation, and failure of the composite wing skins, a composite coupon test campaign was carried out to characterize the material properties of the composite wing skin. This test data feeds directly into the finite element analysis models and margin computations of the wing skins.

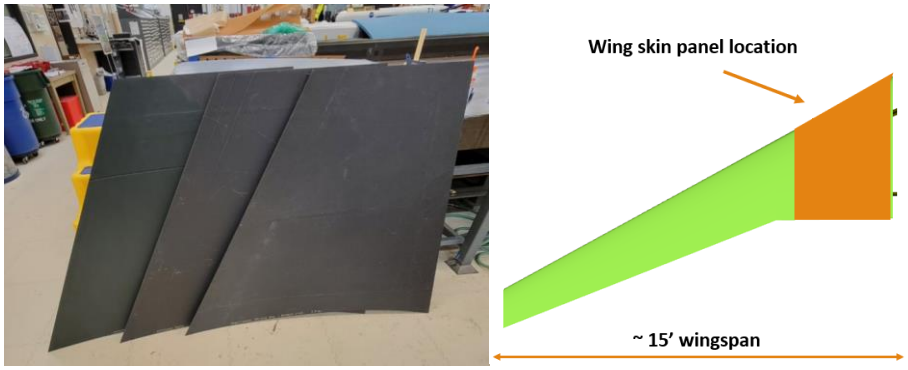

Fig. 9. Manufacturing demonstration wing skin panels shown on left. On right, graphical demonstration of panel size and location on ¼ scale SUSAN wing.

Testing objectives were met and completed which included: tensile and shear testing of varying composite coupon configurations for material characterization. Different coupon configuration allowed for characterization of the wing skin build up regions, main acreage regions, as well as characterizing the two separate composite material systems used. In addition to these composite material systems being used for the wing skins, they will also be used for the flight research vehicle fuselage structure.

Tensile testing followed ASTM D3039 standard practices to determine the in-plane tensile properties of the composite coupons [6]. An example of the test setup and coupon failure locations is shown in Figure 10. 8 coupons were tested per representative panel region/material for a total of 32 tensile coupons. The testing matrix followed with:

- Panel 1: Coupons characterized 2363 material system
- Panel 2: Coupons characterized 530 material system
- Panel 3: Coupons characterized buildup region of wing skin
- Panel 4: Coupons characterized acreage region of wing skin

In plane properties computed and input into the wing skin finite element model include the ultimate tensile strength, modulus of elasticity, and the Poisson's ratio.

Fig. 10. Tensile test setup and example coupon failure locations.

Shear testing followed ASTM D5379 standard practices to determine the in-plane shear properties of the composite coupons [5]. An example of the test setup and coupon failure locations is shown in Figure 11. 5 coupons were tested per representative panel region/material for a total of 15 tensile coupons. The testing matrix followed with:

- Panel 3: Shear coupons characterized buildup region of wing skin
- Panel 5: Coupons characterized 2363 material system shear properties
- Panel 5: Coupons characterized 530 material system shear properties

In plane properties computed and input into the wing skin finite element model include the ultimate shear strength and shear modulus.

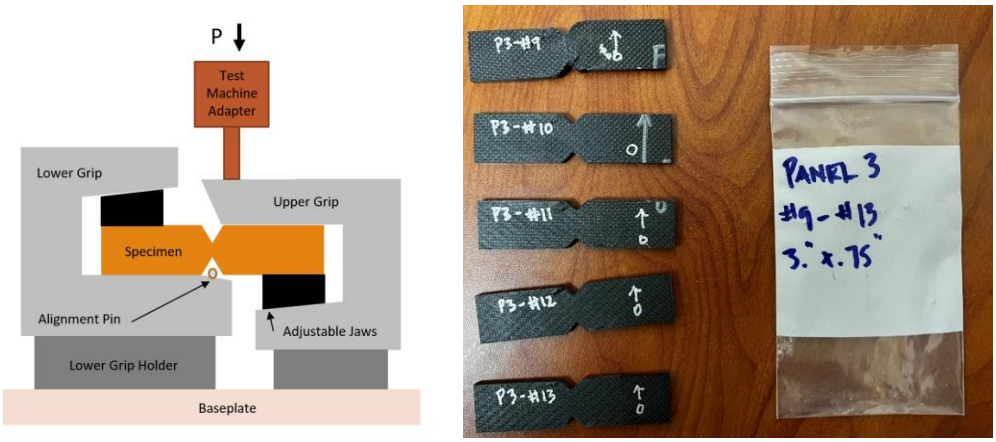

Fig. 11. Shear test setup and example coupon failure locations.

Data quality was checked for all tensile and shear computed properties by looking at the standard deviation and coefficient of variation (CV). The coefficient of variation for all computed values fell in an acceptable range

showing low variability, while most strength and modulus values fell in a very good range with a CV less than 10. The assumed data reporting method here utilizes mean values of all computed properties.

VII. Assembly of Internal & External Wing Structure

The assembly of the wing internal structure with the win skins is such that the wing skins fasten to the ribs which follow the profile of the wing OML. The initial design concept of this fastening system can be seen in Figure 12 below which depicts a rib with flanges that provide a connection point to the wing. This layout is based on a structural skin concept. Additional wing structure and composite wing skin analysis is to be completed to determine the appropriate fastening system to be used here to maintain positive margins of safety of the structure as well as fasteners.

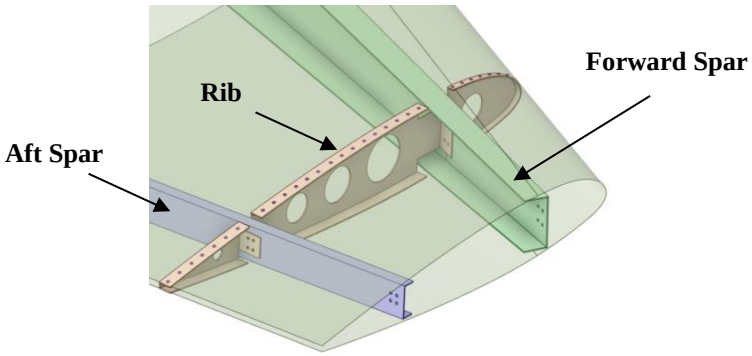

Fig. 12. Rib design concept for connection to wing skins.

VIII. Early Concept of Wing Integration to Plane Fuselage

The integration concept of the wing with the fuselage structure via a separable joint was first explored with the manufacturing demonstration vehicle. The driving factor behind this separable joint concept is the requirement that the SARV structure be transportable. To meet this condition, the design intent is to have two separate wings that will meet in the center to form the wing box, and then attach to the fuselage. Assembly would follow the process of the wing be assembled on the ground, lifted into position, and connected to the fuselage.

Following this design, the wings must connect to the fuselage with a joint that allows for the wings to be easily removed and reattached as needed. The early concept used on the manufacturing demonstration vehicle includes vertical and angled turnbuckle connections from the wing forward and aft spars to the fuselage stringers for a nearly statically determinant joint. An example of this connection is shown in Figure 13 below. Design iterations of this concept are in work to meet both the project separable joint requirements, as well as analysis to ensure the joints ability to carry flight aerodynamic loads.

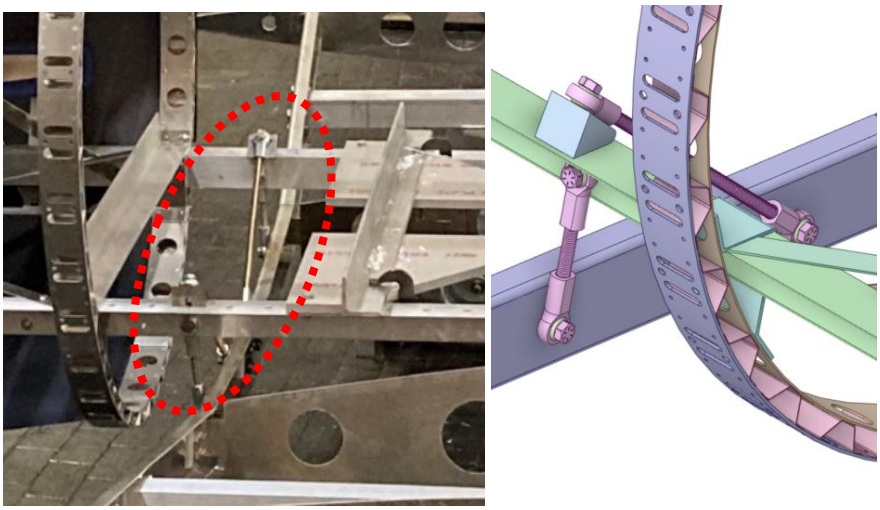

Fig. 13. Separable wing joint concept.

IX. Next Steps

The next steps for the SARV wing structure will look at updating the wing design and analysis for manufacturability considerations and lessons learned from the fabrication of the manufacturing demonstration vehicle. Additionally, with evolving battery box considerations in the wing as well as the need to fit the landing gear near the root of the wing, updates will be made to spar/rib layouts to accommodate these design updates. Battery boxes will need to fit around the wing and wing box compartments and be designed in such a way that they are serviceable. Structural support will also need to be added in the wing to integrate the distributed propulsion onto the wing. As this concept matures and the location of the wing mounted motors are defined, control surfaces will be detailed out in the wing design. Overall, next steps will integrate how to go from a manufacturing mock-up to a workable flight concept that is both serviceable, can be assembled, maintains adequate stress and stiffness, and integrates all design concepts.

X. Conclusion

This paper introduced the high-level overview of the design and development of the SUbsonic Single Aft eNgine (SUSAN) Attritable Research Vehicle (SARV) wing structure. This development included a summary of design evolutions, analysis highlighting weight savings opportunities, fabrication of the vehicle for manufacturing demonstration purposes, design and characterization of the composite wing skins, as well as early concepts for assembly and integration of the wing. Next steps in the development of the wing structure look to integrate the distributed electric propulsion, determine landing gear placement, battery packaging, as well as iterate on the wing to fuselage joint concept. With many of the vehicle's unique features such as battery packaging, wing mounted motors, and separable wing joints are still in early concept phases, the development of the wing structure will continue to iterate to meet these evolving constraints.

XI. Acknowledgments

The Convergent Aeronautics Solutions (CAS) Project, which is part of the Transformational Aeronautics Concepts Program (TACP) in the NASA Aeronautics Research Mission Directorate (ARMD), sponsors this work. The CAS project is managed by Keith Wickman, Kurt Papathakis, and Gerald Welch.

References

[1] Lilia Miller and Ralph Jansen. "Structural Requirements for Design and Analysis of 25% Scale Subsonic Single Aft Engine (SUSAN) Research Aircraft," AIAA 2023-1939. AIAA SCITECH 2023 Forum. January 2023.

[2] Kiris, C., Housman, J., Barad, M., Brehm, C., Sozer, E., and Moini-Yekta, S., "Computational Framework for Launch, Ascent, and Vehicle Aerodynamics (LAVA)," Aerospace Science and Technology, Vol. 55, URL: https://www.semanticscholar.org/paper/Computational-framework-for-Launch%2C-Ascent%2C-and-Kiris-Housman/61f2648528d12d544230557b5f909317aee866ac [retrieved 16 November 2022].

[3] National Aeronautics and Space Administration, “Structural Design and Test Factors of Safety for Spaceflight Hardware,” NASA-STD-5001B, 2016.
[4] National Aeronautics and Space Administration, “Aircraft Structural Safety of Flight Guidelines,” AFPR-7123.1-001.
[5] Standard Test Method for Shear Properties of Composite Materials by the V-Notched Beam Method, ASTM D 5379/D 5379M-12 (2012). American Society for Testing and Materials, West Conshohocken, PA.
[6] Standard Test Method for Tensile Properties of Polymer Matrix Composite Materials, ASTM D3039/D3039M – 17 (2017). American Society for Testing and Materials, West Conshohocken, PA.